Article

Sea Level Rise Effect on Groundwater Rise and Stormwater Retention Pond Reliability

Rahman Davtalab [1] , Ali Mirchi [2,*], Rebecca J. Harris [1], Mark X. Troilo [1] and Kaveh Madani [3,4]

[1]   Singhofen and Associates Incorporated, 11723 Orpington St., Orlando, FL 32817, USA;
      rdavtalab@saiengineers.com (R.D.); rebecca.harris@saiengineers.com (R.J.H.);
      mxt@saiengineers.com (M.X.T.)
[2]   Department of Biosystems and Agricultural Engineering, Oklahoma State University, 111 Agricultural Hall,
      Stillwater, OK 74078, USA
[3]   Centre for Environmental Policy, Imperial College London, London SW7 2AZ, UK; k.madani@imperial.ac.uk
[4]   Department of Physical Geography, Stockholm University, SE-106 91 Stockholm, Sweden
[*]   Correspondence: amirchi@okstate.edu

Abstract: The coastal areas of Florida, United States, are exposed to increasing risk of flooding due to sea level rise as well as severe hurricanes. Florida regulations suggest constructing stormwater retention ponds as an option to retain excess runoff generated by the increased impervious area and to protect the environment by reducing pollutants from new developments. Groundwater level rise can significantly lower the soil storage capacity and infiltration at retention ponds, in turn, reducing the pond's capacity to capture consecutive storms due to longer pond volume recovery time. Partial groundwater inundation can affect retention ponds' ability to decrease peak flow rates and keep the post-development outflow lower than or equal to pre-development conditions. In this paper, the reliability and performance of a retention pond near Tampa Bay, Florida, was evaluated under sea level rise conditions. An integrated surface water and groundwater model was developed, and the groundwater table was projected for future conditions as a function of sea level rise. The results showed that sea level rise could increase the seasonal high water elevation of the retention pond up to 40 cm by mid-21st century. This increase lowered the reliability of the retention pond by about 45%. The pond failed to recover the designed treatment volume within required 72 h because of the high groundwater table, increasing the risk of pollutant discharge. Furthermore, the peak flow and volume of runoff significantly increased under sea level rise and associated groundwater table rise conditions. The study results suggest that it is imperative to consider future sea level rise conditions in stormwater design in low-lying coastal areas of Florida and around the world to prevent poor pond performance and increased risk of flooding in the future.

Keywords: sea level rise; groundwater; retention pond; reliability; Florida

1. Introduction

Global warming leads to ocean thermal expansion and melting of ice sheets in Greenland and Antarctica and consequently causes sea level rise (SLR) [1]. The observed data support an increase of about 1.7 mm/year in the average global sea level rise in the 20th century, which is projected to increase about one more meter by the end of the current century [2]. Local SLR can be much more than these global averages. For instance, the local sea level rise rate is estimated to be about 4.4–8.8 mm/y in Murgia and Salento in Southern Italy [3]. The National Climate Assessment (NCA) reported that sea levels may rise up to 2 m along the United States coastlines by 2100 [4]. Local sea level rise estimates for Acapulco, Mexico, Manila, Philippines, and in Chomklao, Thailand are 7.5 mm/y, 14 mm/y, and 16.5 mm/y, respectively [5–7].

Most of the studies on climate change and flooding issues have addressed anthropogenic changes of rainfall intensity and frequency as well as land-use changes due to development and urbanization [8–10]. These changes substantially alter the peak flow, volume, and duration of flooding and exacerbate domestic inundation areas [11]. In addition to impacts due to rainfall and land-use changes, there is a significant marine flooding risk to highly-populated low-lying cities in coastal areas, including major economic centers such as London, New York, Shanghai, and Mumbai [12]. Globally, it is estimated that more than 20 million people live below the normal high tide elevation and more than 200 million people are under threat of extreme sea level events caused by storms [12]. The United States National Oceanic and Atmospheric Administration (NOAA) reports that about 3.2 billion people worldwide live and work within 200 km of a coastline [13,14], which can be adversely affected by SLR-related closure of access roads and reduced functionality of other infrastructure.

In the United States, the state of Florida ranked 3rd for the number of National Flood Insurance Program (NFIP) claims in the last four decades [15]. The average SLR in Florida for two time horizons, namely 2060 and 2100, are estimated to be about 0.76 m (2.5 feet) and 1.95 m (6.4 feet), respectively [4]. Meanwhile, about 10% of Floridians live in areas with a ground elevation below 1.5 m [16]. Senate Bill (SB) 1094 was passed in 2015 by the Florida legislature to consider the future flood risk from storm surge and sea level rise in certain portions of local government master plans. Nevertheless, stormwater system design in the state is still, generally, based on assumptions of stationary sea level conditions, although the need for accounting for nonstationary future conditions in hydrologic analyses has been recognized [17–19]. The cost increases associated with designs that account for SLR and the combined effects of SLR and rainfall increase are significantly lower when compared to the cost to retrofit a system after construction [20].

Retention ponds are an integral component of stormwater management plans in Florida, as well as many other areas. Retention ponds help protect the infrastructure and ecosystems in coupled natural-human systems. They are typically designed to maintain the predevelopment runoff condition by detaining the outflow or infiltrating the additional runoff generated by impervious areas, and by providing pollutant removal through settling and biological uptake [11,21]. The outlet structure for retention ponds is designed to provide complete storage and percolation of a specified treatment volume to remove pollutants.

This study examines how the reliability of stormwater retention ponds in regulating runoff and removing pollutants can be affected by groundwater changes due to SLR. SLR can increase groundwater-related flooding by raising groundwater tables [22–24]. The loss of percolation capability due to reduced infiltration and subsurface storage because of high groundwater tables can have a significant impact on the treatment capacity provided by a retention system. Using a case study from Tampa Bay, Florida, we demonstrate the importance of accounting for SLR-related higher groundwater tables in the design of retention ponds to prevent poor performance in the long run.

2. Study Area and Regulatory Framework

The study area covers 49 hectares (122-acres) in the Southwest Florida Water Management District (SWFWMD). The project area is connected to Tampa Bay, which is classified as impaired, and, ultimately, the Gulf of Mexico to the southwest (Figure 1). Florida has enacted some of the most restrictive environmental requirements in the United States to protect its water resources and natural habitats. New development is often regulated through the state's Environment Resource Permit (ERP) requirements. The Florida Department of Environmental Protection (FDEP) has delegated this responsibility to regional water management districts.

Two major regulations must be followed to obtain an ERP for a new development [25]. First, stormwater pollutant removal must be provided prior to discharging project runoff off-site, including discharge to public drainage systems or other water bodies, to ensure the new development does not increase pollutant loads. Second, off-site peak discharge for the post-development condition should not exceed pre-development discharge from the property. SWFWMD allows an exemption for

the pre- and post-discharge requirement when the receiving point is a tidal water body, such as the Gulf of Mexico. In this situation, there is no requirement on peak rate of discharge. Since the discharge point for this study has about 1.5-km (~1 mile) distance to the Bay and is not directly discharging to it, the peak rate requirements for retention pond design were considered. The off-site discharge is typically estimated using the rate of discharge for 25-year, 24-h storm for open basins and the volume discharge for 100-year, 24-h storm for closed basins.

There are multiple ways to address these requirements. The treatment volume is determined based upon the methodology chosen for the project, which depends on soil and groundwater conditions at the project site. Two of the most commonly used approaches are retention- and detention-based methodologies. Retention methodology, which is applied in this study, provides storage of the treatment volume and recovery of that storage through percolation or evaporation over several days. Detention provides temporary storage of the treatment volume in a pond equipped with a control structure and bleed-down device that slowly releases the treatment volume to surface water over several days. Based on the ERP [25], the required treatment volume for the considered project is one inch (2.54 cm) over the entire development area. This volume must be recovered within 72 h, so the treatment volume is available to capture and treat runoff from subsequent storms. The total outflow for existing and post-project conditions are evaluated to illustrate the performance of the pond under these two conditions.
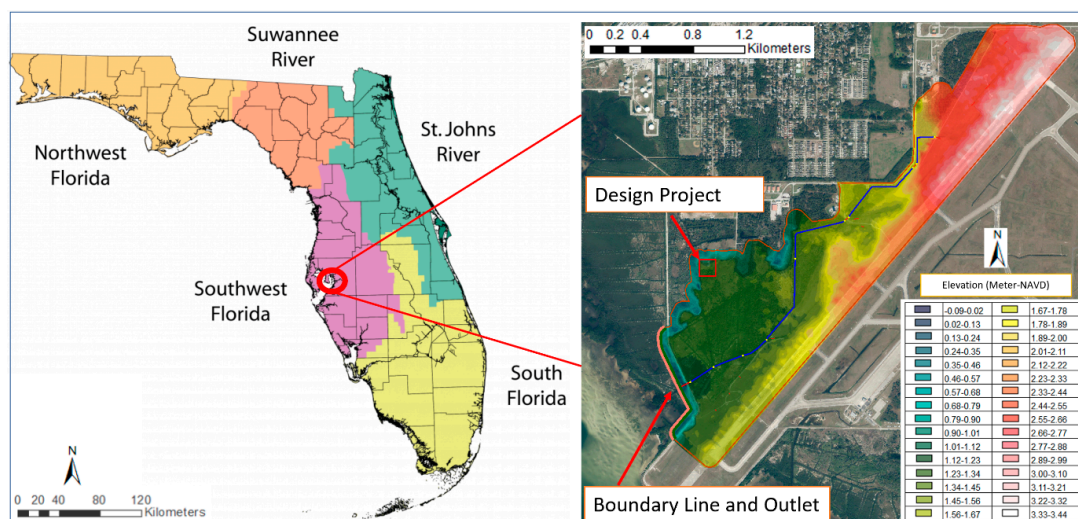

Figure 1. Location of project area in Southwest Florida.

3. Input Data

Primary input data include rainfall, evapotranspiration, soil properties, land-use map, and tide data. Long-term rainfall data from Next Generation Weather Radar (NEXRAD) was used in this study to perform a continuous simulation of the pond's performance under SLR. Calibrated 15-min NEXRAD rainfall data are available on a 2-km grid [26]. Atlas 14 rainfall intensity data [27] and the Soil Conservation Service (SCS) Type II Florida Modified rainfall distribution were used for synthetic design storm simulations. Based on Atlas 14, the 25-year, 24-h rainfall for the study area is about 21 cm. The potential evapotranspiration (PET), which is a significant loss in continuous simulations, was obtained from United States Geologic Survey (USGS). The PET data were provided in the same spatial grid as the NEXRAD data on a daily time scale.

The soils zone map and related parameters for modeling infiltration using the Green–Ampt method (e.g., porosity and hydraulic conductivity) were obtained directly or based on data from the National Resources Conservation Service database [28]. The majority of the project site has good soils with high infiltration and high porosity (Figure 2a and Table 1). The groundwater table, however, is relatively close to the ground surface, especially in the Tampa Bay area. Land-use data available from

the SWFWMD were used along with post development land-use for developing TR-55 [29] impervious area lookup tables (Figure 2b). Existing land-use on the project site consists of mixed hardwood conifer and open land. Post development land-use conditions include commercial building space, parking lot, and a new retention pond.

The Manning's roughness values were also determined based on the land-use analysis for use by the surface water model (see Section 4.1). Two different Manning's n values were applied for representing shallow flow (i.e., up to 0.914 m (3 ft)) and deep flow (i.e., greater than 0.914 m) conditions to capture greater roughness close to the ground surface in shallow flow compared with deep waters, which will have smaller Manning's roughness values. The study area is mostly covered by dense tidal marsh plants and brushes close to the ground surface. The density of the canopy declines as the elevation increases, typically reaching about 0.914 m above the ground level, which is the basis for the depth threshold for applying deep Manning's roughness coefficient. The model generates vertically varied Manning's n values up to 0.914 m above the ground elevation based on an exponential equation using the specified shallow and deep flow Manning's n values [30]. Deep flow Manning's roughness coefficients are used when the flow depth exceeds the 0.914 m threshold. Table 2 shows the Manning's roughness values for different land-use types.

Tide data for a nearby Tampa Bay gage (station ID 8726520) were obtained from NOAA to set the sea level boundary conditions for this study. The mean high water elevation (MHW) is 0.6 m (1.98 feet), above the mean lower low water elevation (MLLW), which is 0.15 m based on North American Datum of 1988 (M-NAVD-88). For surface water/groundwater modeling and the SLR study, ground elevation plays a key role. Therefore, a 1.5 m LiDAR-based digital elevation model (DEM) was used in this study. The FDEP has data for various hydrogeologic components including Florida Aquifer Units (FAU) and potentiometric surface, which were also used in this study. The projected SLR for a time horizon of 2060 is about 79 cm (2.6 feet), which was determined from NCA [4] to adjust tailwater for the future conditions simulation.
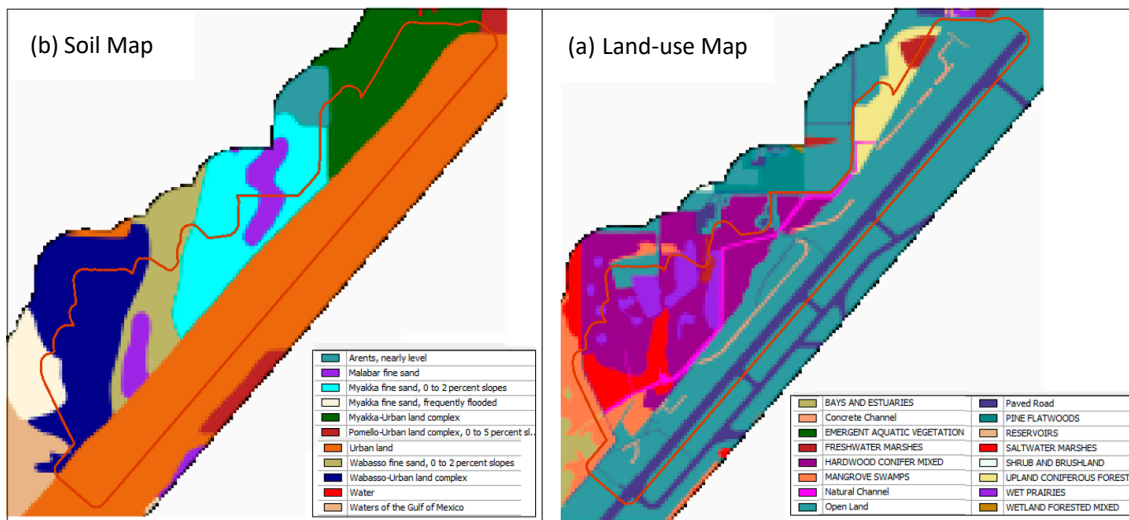

Figure 2. Natural Resource Conservation Service (NRCS) soil map (**a**) and SFWMD land-use map (**b**).

Table 1. Green–Ampt soil parameters from Natural Resource Conservation Service (NRCS) data base.

Soil Zone	Kv Sat. (m/d)	MC Sat.	MC Res.	MC Init.	MC Field	MC Wilt.	Pore SI	Bubble Press (cm)
Arents, nearly level	4.0	0.451	0.018	0.091	0.091	0.035	0.502	2.7
Malabar fine sand	3.2	0.419	0.018	0.091	0.091	0.036	0.506	3.2
Myakka fine sand, 0%–2% slopes	3.4	0.416	0.020	0.099	0.099	0.039	0.552	3.8
Myakka fine sand, frequently flooded	3.4	0.455	0.024	0.121	0.121	0.048	0.549	2.8
Myakka-Urban land complex	3.6	0.407	0.009	0.051	0.051	0.018	0.575	3.7
Pomello-Urban land complex, 0%–5% slopes	6.2	0.435	0.006	0.036	0.036	0.011	0.560	3.2
Urban land	4.0	0.443	0.002	0.009	0.009	0.004	0.505	2.8
Wabasso fine sand, 0%–2% slopes	3.4	0.434	0.036	0.151	0.151	0.072	0.465	3.4
Wabasso-Urban land complex	3.0	0.409	0.014	0.067	0.067	0.027	0.478	3.9

Note: Kv Sat: saturated vertical hydraulic conductivity; MC Sat: saturated moisture content; MC Res: residual moisture content; MC Init.: initial moisture content; MC Field: moisture content at field capacity; MC Wilt: moisture content at wilting point; Pore SI: pore size index; Bubble Press: bubble pressure.

Table 2. Shallow and deep Manning's roughness coefficient (n) for 2D surface model (based on Chow [31] and TR-55 [29]).

| Roughness Zone	Shallow Manning's n	Deep Manning's n
Bays and Estuaries	0.060	0.030
Concrete Channel	0.060	0.030
Emergent Aquatic Vegetation	0.300	0.200
Freshwater Marshes	0.300	0.200
Hardwood Conifer Mixed	0.400	0.200
Mangrove Swamps	0.300	0.200
Natural Channel	0.100	0.080
Open Land	0.150	0.040
Paved Road	0.014	0.012
Pine Flatwoods	0.300	0.200
Reservoirs	0.300	0.200
Saltwater Marshes	0.300	0.200
Shrub and Brushland	0.300	0.150
Upland Coniferous Forest	0.400	0.200
Wet Prairies	0.300	0.200
Wetland Forested Mixed	0.400	0.200

4. Modeling Framework

4.1. Hydrologic and Hydraulic Model Structure and Components

An integrated surface water and groundwater model was developed to evaluate the effects that SLR-related groundwater changes may have on the performance and reliability of retention pond functions. The Interconnected Channel and Pond Routing (ICPR) model [30], which includes a fully-integrated 1D/2D surface water module coupled with a 2D groundwater module was applied. The coupled model allows interaction between surficial aquifer systems and surface water bodies.

Figure 3 shows the general structure and major features of an ICPR 2D model. ICPR has a pre-processer for mesh generation as well as a scenario builder that must be executed before the simulation is conducted. The model generates triangular meshes for both surface water and groundwater calculations and parameterizes all components for the simulation. Several of the 2D features in ICPR, such as pond control volumes and channel control volumes, force the creation of vertices (2D nodes) along their respective polygons during mesh creation.
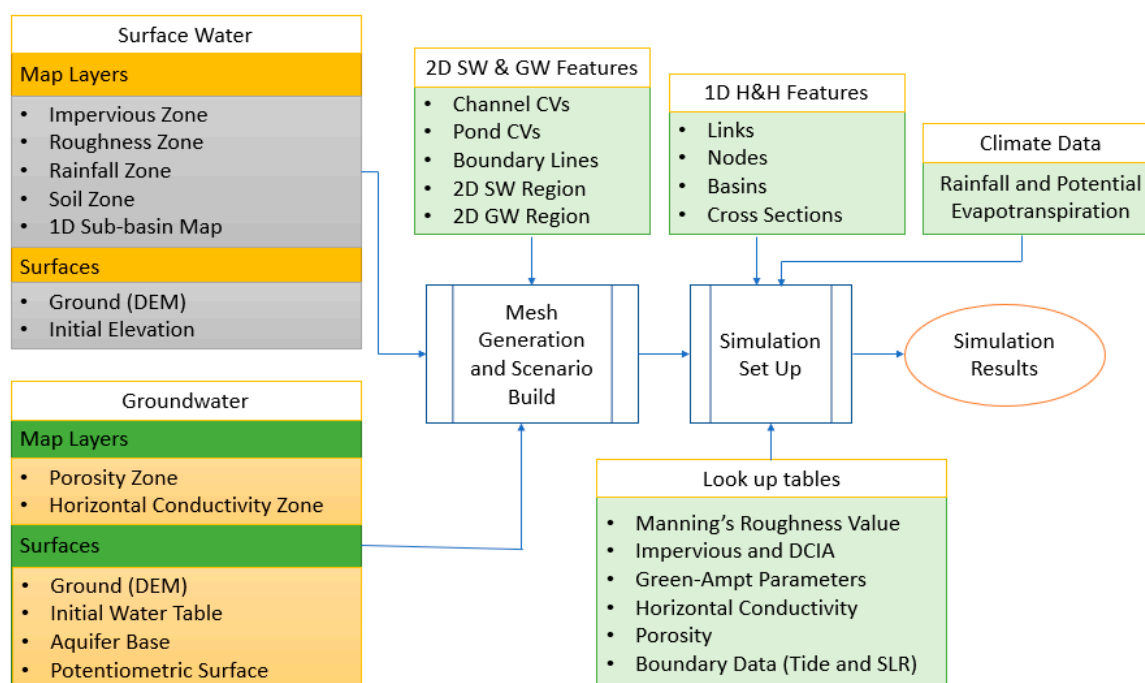
Figure 3. General structure and primary features of the ICPR 2D model. DEM, digital elevation model; H&H, hydrologic and hydraulic; DCIA, directly connected impervious area; SLR, sea level rise; SW, surface water; GW, groundwater; CV, control volume.

The scenario builder uses various map layers and surfaces with the mesh, honeycombs and triangles to calculate the parameters required by each 2D link (triangle sides) and 2D node (vertices) for the hydrologic and hydraulic (H&H) calculations. During the simulation process, the model reads parameters like roughness values, impervious percentage, and hydraulic conductivity from lookup tables related to each map layer. Climate data and 1D H&H input data are independent components of an ICPR model and they can be added to the model database after 2D scenario building before simulation.

For surface water, the initial ground condition was assumed to be dry and the initial elevation was the same as the ground elevation. For groundwater, the initial water table elevation was estimated based on a digital elevation model (DEM) and water table information from the NRCS soil database. It should be noted that for continuous simulations, a "warm-up" run was executed for a couple of months to allow the initial water table to stabilize. The warm-up simulation was then used as a "hot

start" for the continuous simulations. The average of wet season water elevations (June through October) was used as the initial water table for discrete event simulations.

4.2. Excess Rainfall, Infiltration, and Groundwater

Both event-based simulations and continuous simulations were considered in this study. The Green–Ampt method [32] provided in ICPR is a useful rainfall-runoff method that allows water tracking during hydrologic simulations throughout the soil column, including dry and wet periods. The Green–Ampt method is based on Darcy's law:

$$q = -k_v I, \tag{1}$$

where k_v is the vertical hydraulic conductivity (m/day) and I is the gradient defined as the summation of ponding head (H), saturated wetting front below the ground (Z_f), and the capillary suction head (h_c) as shown in Figure 4.

$$I = \left(H + Z_f + h_c\right)/Z_f, \tag{2}$$
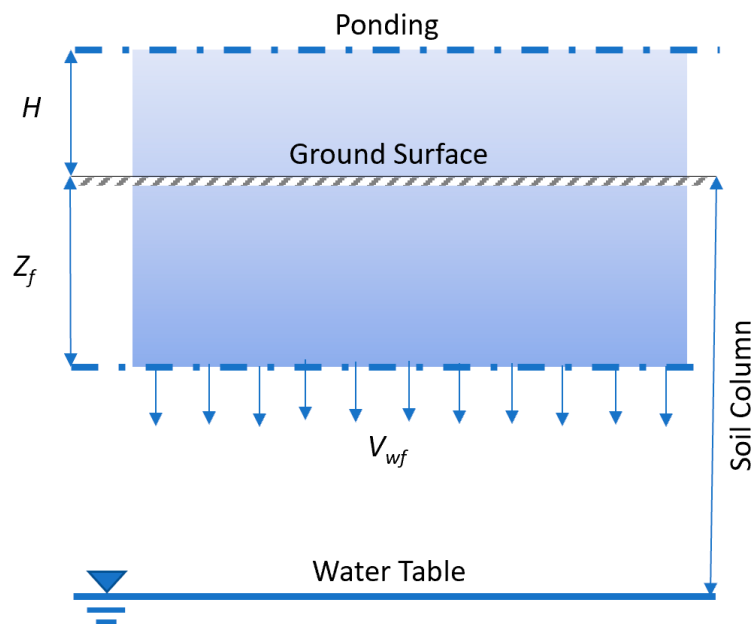
Figure 4. Governing factors for vertical water movement in the Green–Ampt method. *H, ponding head*; Z_f, saturated wetting front below the ground; V_{wf}, velocity of wetting front.

ICPR estimates h_c based on moisture content and bubble pressure from soil data (Table 1). Velocity of the wetting front is estimated using the following equation:

$$V_{wf} = dZ_f/dt = q/n, \tag{3}$$

where n is the fillable porosity.

Integrating Equation (3) for time 0 to t_0 and Z_f between 0 to Z_0 yields:

$$\frac{K_v t_0}{n(H + h_c)} = \frac{z_0}{(H + h_c)} - \ln\left(1 + \frac{Z_0}{H + h_c}\right), \tag{4}$$

Equation (4) is used to simulate decay of the infiltration rate. Z_0 is the maximum amount of water that can infiltrate and excess water above the ground represents rainfall excess or ponded storage. In reality, rainfall is not always sufficient to saturate the soil column and evapotranspiration

(ET) can become a significant loss term. Therefore, ICPR uses a modified Green–Ampt method which is explained in the ICPR user manual [30]. Vertical water movement is only conveyed through unsaturated soil zones and horizontal conductivity is applied for water transfer in saturated soil zones. Evapotranspiration is allowed on the surface to the root depth zone which can be defined in the ICPR model. Deep percolation can also be considered, including use of the potentiometric surface data to provide estimates of gradient and leakance, although leakance was not considered in this study (see Section 4.5).

4.3. One-Dimensional Surface Water Components

The ICPR 1D surface model has three primary features: nodes, links, and basins. The basin feature represents areas that contribute runoff to nodes and require a number of parameters for excess rainfall and routing calculations, including basin area, impervious and directly connected impervious area (DCIA), time of concentration, etc. Basins are used for loading of 1D nodes. Areas modeled using 2D surfaces do not require basin features (2D surface modeling is explained in the next section). A basin is associated with a node. Nodes represent locations in the model where mass balance is tracked and are used to represent ponds or drainage system junctions; the storage data for a node is typically contained within the basin assigned to that node. Runoff transfers from one node to another node through links which represent water conveyance features such as culverts, channels, overland flow weirs or other types of hydraulic connections. ICPR has three options for flow rate calculations through channels and pipes: the energy equation, the momentum equation, and the diffusive wave equation [30]. The energy method was used for flow calculations in this study:

$$Z_1 + \frac{\alpha_1 V_1^2}{2g} = Z_2 + \frac{\alpha_2 V_2^2}{2g} + h_f + h_{eddy} + h_{entrance} + h_{exit} + h_{bend}, \tag{5}$$

where subscripts 1 and 2 represent conditions at nodes 1 and 2, respectively; Z represents elevation (m); α_1 and α_2 are energy loss coefficients; V represents velocity (m/s); g is gravitational acceleration (m/s^2); h_f is the friction loss coefficient; h_{eddy} is an eddy loss coefficient; $h_{entrance}$ is an entrance loss coefficient; h_{exit} is an exit loss coefficient and h_{bend} is a bend loss coefficient.

Equation (5) is solved for velocity to obtain Q as follows:

$$Q = \left\{ \frac{Z_1 - Z_2}{\frac{1}{2g}\left[\frac{\alpha_2}{A_2^2} - \frac{\alpha_1}{A_1^2} + C_{eddy}\left|\left(\frac{\alpha_1}{A_1^2} - \frac{\alpha_2}{A_2^2}\right)\right| + \left(\frac{\alpha_1 C_{entrance}}{A_1^2}\right) + \left(\frac{\alpha_2 C_{exit}}{A_2^2}\right) + \left(\frac{\alpha_{bend} C_{bend}}{A_{bend}^2}\right)\right] + \Delta x C_f} \right\}^{1/2}, \tag{6}$$

where Q is flow (Velocity × Area); A_1 and A_2 are cross sectional areas at node 1 and node 2, respectively; C represents different loss coefficients of eddy, entrance, exit, bend, and friction, and Δx is the length between nodes in the X-direction.

There are other links like weir or orifice which have specific equations for flow rate calculations [33]. The 1D portion of the H&H model in this study includes about 3 km of channels extending from the northeast all the way to the southwestern bay area and about 370 m of cross-drain concrete pipes along the way (Figure 1).

4.4. Two-Dimensional Surface Water Components

ICPR's two-dimensional overland flow option can be applied for surface water simulation. In this method a flexible triangular computational mesh is used to simulate overland flow instead of using "traditional" lumped basins and 1D node/link networks. The 2D approach implemented in ICPR treats the triangle vertices of the mesh as 2D nodes and the sides as 2D links. The mesh is constructed semi-automatically using a number of features to "fine tune" the mesh to represent ridge lines and

flow ways. The mesh is normally created with a much higher resolution than would be practical using 1D features alone.

ICPR automatically generates a "honeycomb" and "diamond" network of polygons during mesh construction. The honeycombs are centered around each of the triangle's vertices and are analogous to catchments or basins in a 1D model (Figure 5). Hydrologic parameterization of the honeycombs is performed in essentially the same manner as for 1D basins. The diamonds are centered around the 2D links and are used to calculate overland flow hydraulic properties.
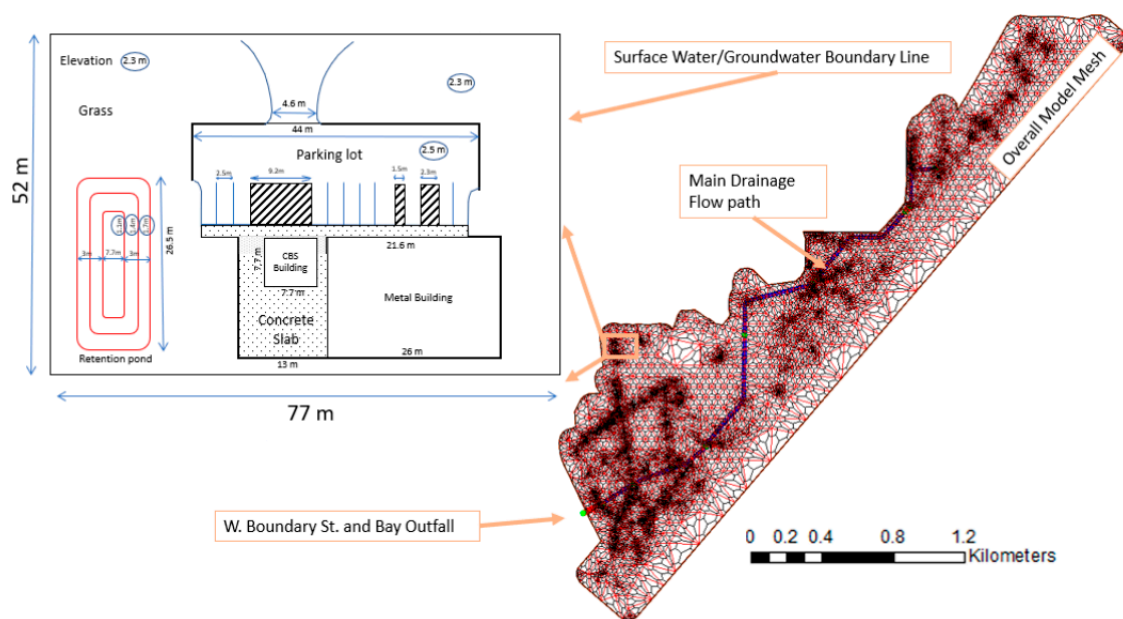
Figure 5. Groundwater/surface water computational meshes for model domain (left) and project site (right).

A series of lookup tables (e.g., rainfall excess and Manning's roughness) are used to specify parameter values for the H&H parameterization. DEM and polygon map layers of roughness, impervious areas, soils, and rainfall zones are imported into ICPR. The map layers and lookup tables, through the Scenario Build tool, are used to generate the required parameters for H&H calculations in the mesh area.

ICPR applies a special case of Equation (5), which only includes hydraulic head and friction and velocity losses for water transfer between the 2D nodes and through the links. Water may move between the 2D surface and 1D channels or 1D ponds. This water transfer is carried out at vertices along special 2D features known as channel control and pond control volumes. The overland flow region boundary alone serves as a "glass wall" and surface water is not permitted to pass through it, however, boundary stage lines along the region or 1D links with connections to a boundary node can be provided to allow water to leave the model domain or otherwise interact with upstream or downstream boundary conditions (i.e., water bodies with known elevations).

Tide-affected areas of Tampa Bay serve as the tailwater. Discharge from the downstream end of the system is through a double barrel 91 cm concrete pipe to the bay outfall (Figure 5). In addition, a boundary stage line with the same time stage data was provided for boundary conditions along tidal 2D areas of the model. For continuous simulation, the varied tide data and varied projected tide data (i.e., projected per SLR) were used for the time series boundary data under current and future conditions, respectively. For discrete events or synthetic storm simulations, a fixed value of Seasonal High Water (SHW) was used for current and future conditions at the time/stage boundary node.

4.5. Two-Dimensional Groundwater Components

The two-dimensional groundwater component of ICPR is designed to simulate horizontal flow through the surficial aquifer, vertical leakance through the confining layer, and seepage into channels, ponds, and depressions. Darcy's law is the basis for these simulations. Like 2D surface modeling, the 2D groundwater module uses a flexible computational triangular mesh (Figure 5). The triangles are intersected with porosity and conductivity zone polygon map layers to estimate average porosity and conductivity. Triangle nodes are intersected with different surfaces, such as the ground, confining layer, initial water table, and potentiometric elevation for extracting the required parameters. Deep percolation or leakance is allowed in ICPR and the potentiometric surface can be used to estimate gradients and amounts of leakance. Since leakance is significantly lower than horizontal and vertical conductivity, and assuming it is constant for existing and future conditions, it was not considered in the current analysis.

4.6. Impact Assessment Framework

To reduce model run times, a two-stage assessment framework was applied (Figure 6). In the first stage, the ICPR 2D surface and groundwater model was used to conduct continuous simulations for the entire study area, which contains the Tampa Bay project site. In the second stage, a reduced model domain was prepared only for the project site and a small buffer area around it. The study area was simulated under current condition, as well as future SLR-conditions with higher tailwater elevations. The smaller model domain allowed evaluation of different design options and adaptation scenarios with reasonable computational effort while using consistent boundary conditions from the study area simulation. The project site model boundary conditions provided by the continuous simulation results from the study area model, including current and future SHW levels for discrete storm simulations and surface water/groundwater time series data for continuous simulations (Figure 6).
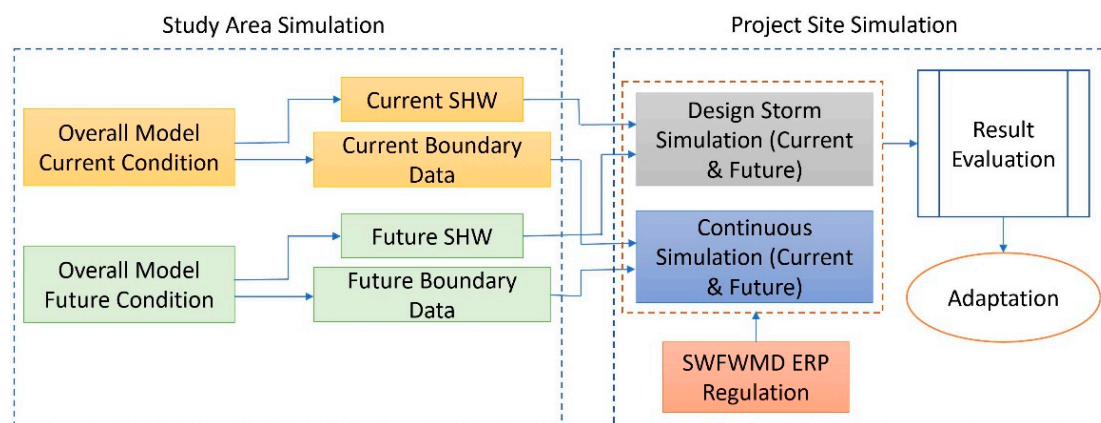
Figure 6. Components of the two-stage impact assessment framework. SHW, seasonal high water.

While the simulations included multiple years, 2012 was selected as a representative year for current conditions to provide a basis for comparing retention pond performance under different SLR and adaptation scenarios. The study area received 113 cm rainfall in 2012, which is close to the long-term average (125 cm). Likewise, the rainfall for the 2012 wet period is close to the long-term average. Tropical Storm Debby dropped about 16.5 cm of rain in the study area between 23 June and 25 June, 2012. However, even if the June rainfall were excluded from the 2012 wet period (i.e., consider July to October only), the wet period rainfall in 2012 remains close to the long term average for the July-October period (58.4 cm vs. 63.5 cm). The dry period rainfall for this year (November–May) was below the long-term average (i.e., 60 percent of the long-term average). However, the focus of this study was on the wet period, when retention ponds are most active. Thus, 2012 was deemed suitable

for baseline analysis because it included an extreme event to examine the performance of the system under a wide range of hydrologic conditions.

An ICPR land use map layer was prepared to reflect post development conditions. Southwest Florida Water Management District's ERP regulatory requirements were used to design the stormwater facility [25]. The stormwater retention pond must store and percolate the first 1″ (2.54 cm) of rainfall over the site as required by SWFWMD. The total area of development (pre and post) is 3966 square meters (or 0.98 acre) and 1″ of rainfall over this area is about 101 cubic meters (or 0.082 ac-ft). Storage for this volume is to be provided by a 364 square meter retention pond with an outlet at elevation of 1.3 M-NAVD-88. The total project area consists of 1619 m^2 (0.4 ac) impervious surfaces (e.g., building, parking, and pavement) while the remaining 1983 m^2 (0.98 ac) is pervious.

Post development hydrologic impact analysis consisted of volume recovery assessment and long-term performance of the retention basin under SLR. Based on ERP requirements, the treatment volume should be recovered within 72 h. A drawdown analysis was conducted using the small project site model for current and future conditions to ensure that the volume recovery requirement is satisfied. The project site model was also used to simulate the 25 year-24 h design storm. A year-long continuous simulation was performed to evaluate performance of the retention pond under representative current and future conditions (i.e., 2012 and 2060). For the annual design storm simulation, the tailwater and groundwater elevation were assumed to be constant and were set to current and future SHW levels as estimated from the study area simulation. For the continuous simulation, the boundary data were varied with time based on results from the study area model.

4.7. Reliability of Stormwater Retention Pond

The reliability of performance of the retention pond was evaluated using the results of the continuous simulation under current and future conditions. The reliability index defined by Hashimoto et al. [34] has been widely used in the water resources management literature [35–39]. In this study, reliability can be defined as the percentage of time that the retention pond is able to fully capture the storm runoff. In other words, any day with at least one-time outflow (regardless of duration), was defined as system failure or unmet target (Equation (7)). The ERP permitting criteria stipulates retention ponds on project sites discharging stormwater to an Outstanding Florida Water (OFW) or impaired waters, must retain more than 95% of storm events.

$$R = \frac{No. \ of \ Fi = 0}{n}, \tag{7}$$

$$F_i = Maximum(0, Peak_i - CELV), \tag{8}$$

where *Peak$_i$*: peak stage for retention pond for day *i*; *CELV*: pond control elevation; *F$_i$* flood depth above control structure for day *i*; and n: number of days which is 365 in the current application.

5. Results and Discussion

5.1. Continuous Simulation

The first set of simulations was completed for the base year of 2012 (current condition) and future year of 2060 with projected tide data as the tailwater. Year 2012 was a normal year including Tropical Storm (TP) Debby, so it was selected intentionally to examine the flexibility of retention pond during the extreme event. It should be noted that Tropical Storm Debby occurred between the 23 and 25 of June 2012 and dropped more than 16.5 cm of rainfall in the study area. The total time for each simulation was 12 h and the total mass balance error was less than 0.5 percent.

The hourly groundwater elevation time series was processed inside the ICPR model to generate median groundwater table elevations for current (2012) and future (2060) conditions. Figure 7 displays these median groundwater elevations for each pixel of the 2D model of the study area, including

the project site. There is a significant change between current and future groundwater conditions, especially in the bay area (Point A in Figure 7), which is most affected by the tide. The black line in this figure is the primary outflow path of the study area. As shown in Figure 8, the discrepancies between groundwater elevations in current and future conditions can be up to 1 m. Another important result depicted in these profiles is that the median groundwater elevation in current conditions is below the ground surface for the majority of the flow path while, under future conditions, the groundwater table is elevated above the ground surface for a significant portion of the profile (Figure 8).
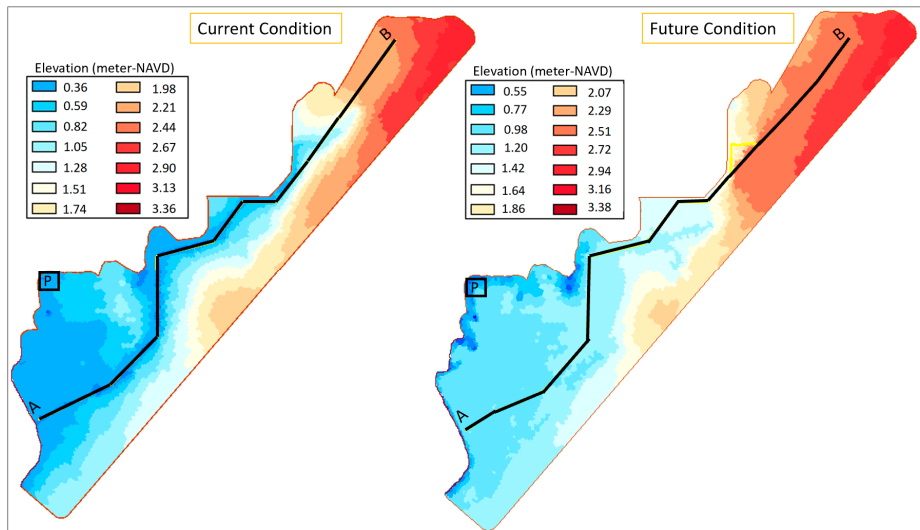

Figure 7. Spatial distribution of median groundwater elevations for current (2012) and future (2060) conditions. P denotes project site. B and A show the start and end of the main drainage flow path (black line), respectively.
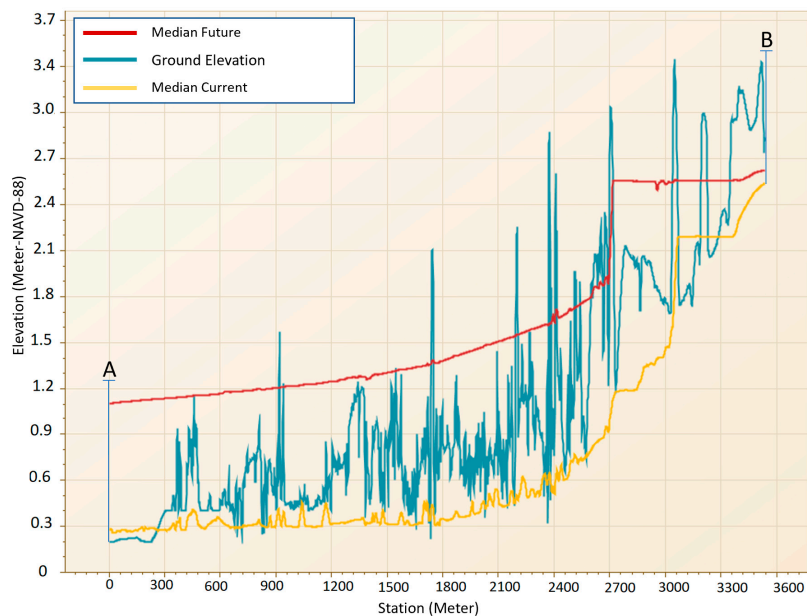
Figure 8. Comparison of ground surface elevation and median current and future groundwater profiles along the primary outflow path in the study area. B and A represent the start and end of the primary outflow path, respectively.

Figure 9 displays the groundwater elevation at the project site for current and future conditions. The two groundwater elevation time series plots in this graph were used as boundary data (or tailwater)

for the project site model (i.e., stage 2 of the impact assessment framework). Figure 9 also shows the average groundwater elevation for the project site during Florida's wet season, namely the five months that span from June through October. This average is known as the seasonal high water level (SHW), which is a constraint for retention system design and analysis in Florida. Based on this figure, the SHW at the project site increased from 0.8 M-NAVD in current conditions to 1.2 M-NAVD in future conditions in 2060.
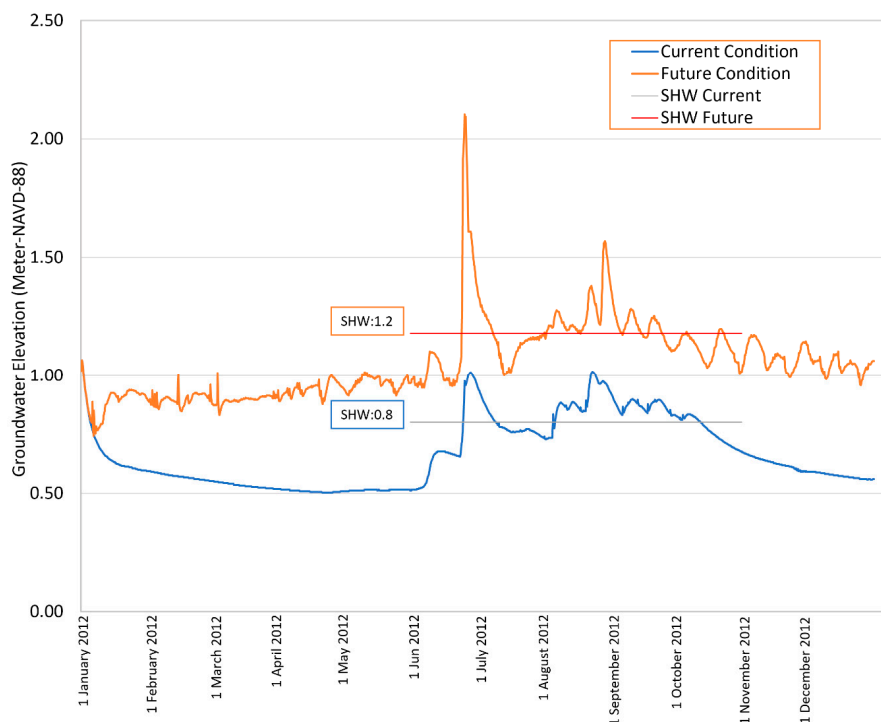
Figure 9. Groundwater elevation and SHW at project location for current and future conditions.

5.2. Retention Pond Performance

For drawdown analysis of the retention pond for current and future conditions, the pond's initial water elevation was set to the top of the treatment volume and the boundary data were set to the fixed SHW of 0.8 m and 1.2 M-NAVD-88 for current and future conditions, respectively. The model was simulated for 72 h without any rainfall. Figure 10 shows the recovered volume for the current and future conditions. The stormwater retention pond recovers the treatment volume (101 cubic meters) within 26 h in current conditions, meaning that the retention pond meets the required water quality criteria. The storage recovery under future conditions indicates that the retention pond will only recover 79 cubic meters of its required stormwater capture volume after 72 h. In this case, the retention pond does not comply with SWFWMD's requirements, which are those used in the permitting process. In other words, although the designed retention pond fully meets the permitting requirements under current conditions, it fails in important ways to meet the same requirements in 2060 when impacts of SLR on groundwater table are accounted for in the analysis.

Under the 25-year, 24-h design storm (about 21 cm), which is the basis for designing most stormwater facilities in the SWFWMD, the peak discharge flow rate for current and future conditions are 52 L/S and 76 L/S, respectively. Therefore, the projected peak flow increase for future conditions is about 47%. The peak discharged volume for current and future conditions are estimated as 143 and 288 cubic meter, respectively. Therefore, the discharged volume for future condition is more than 100% greater than current condition.

The pond's reliability was also analyzed under peak flows and fixed SHW. A strict rule was used for reliability calculations whereby a day is considered a failure if the pond has an outflow anytime

during the course of that day. The pond has an outflow anytime the water elevation is higher than the control elevation. Figure 11 illustrates the pond's water elevation under current and future conditions and the outlet invert elevation 1.3 M-NAVD, which is used as the control elevation. The results showed that under current conditions, the reliability of the retention pond is more than 99%, meaning that the pond caught and contained the runoff from the system over 99% of the time (i.e., 362 days) in 2012. Conversely, results also showed that the reliability of the stormwater pond decreased to 54% in future conditions, which is a significant drop. Of the 168 failure days (i.e., pond outflow > 0) under future condition, the outflow exceeded pre-development runoff during 160 days. These results suggest that a pond that was permittable under current conditions will be much less reliable, even unpermittable, when considering SLR in the mid-century.
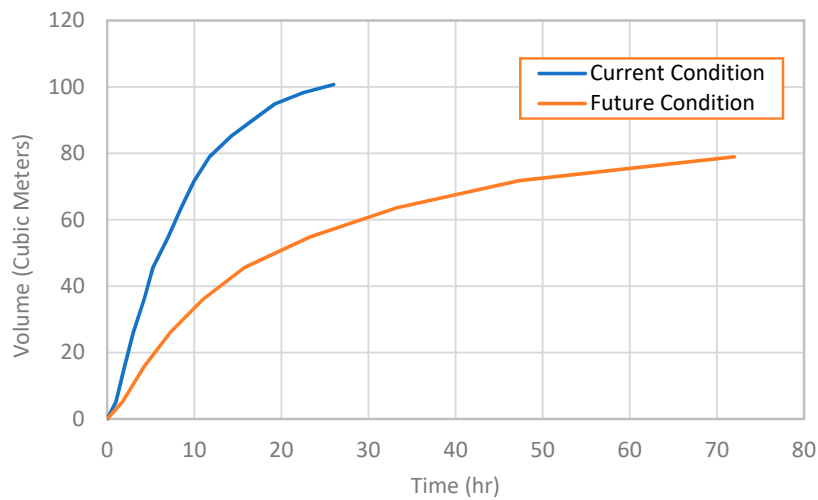

Figure 10. Recovered treatment volume for the current and future conditions.
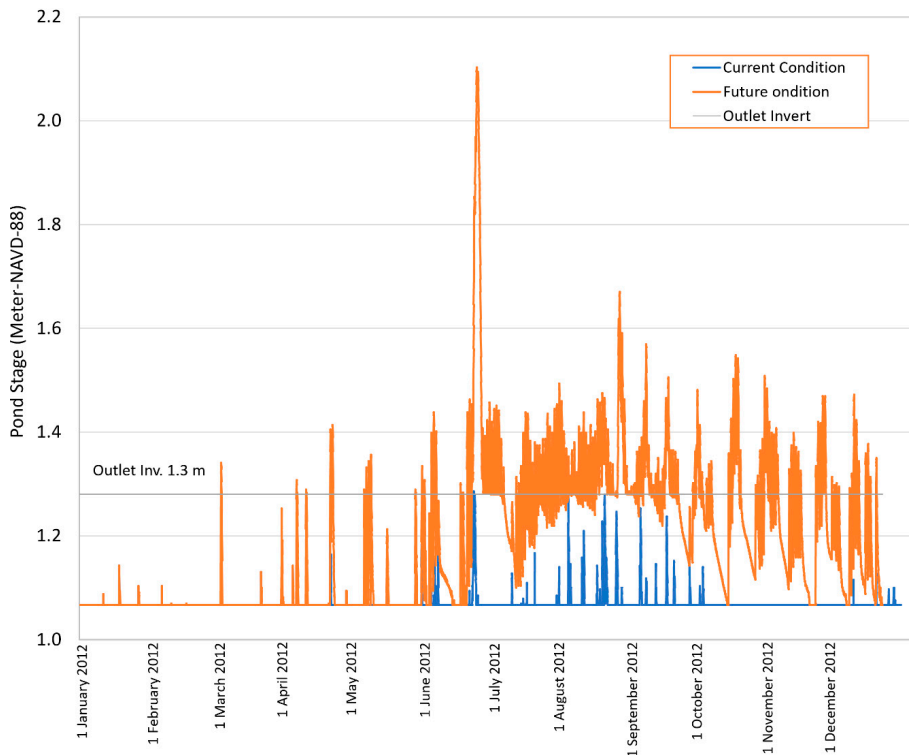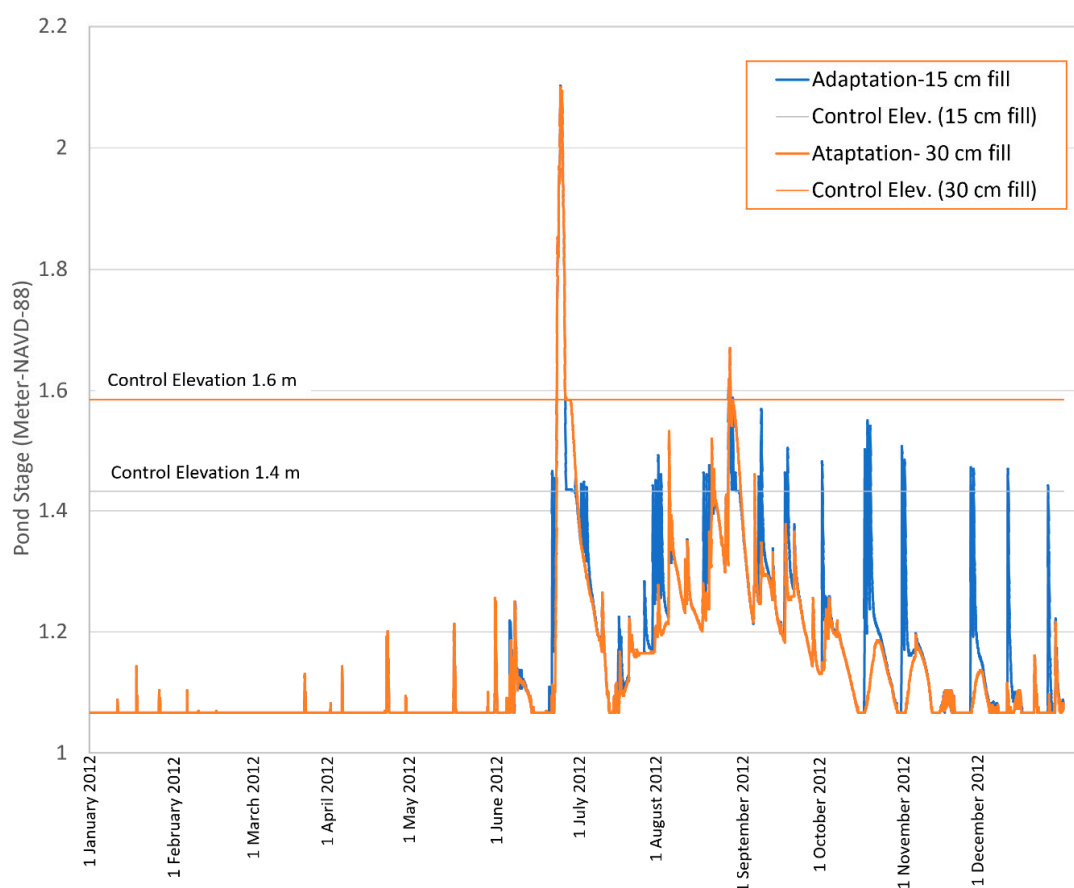

Figure 11. Pond water elevation under current and future conditions.

5.3. Adaptation Scenario

Several methods can be used to improve the performance of a stormwater system in areas of high groundwater table. Low Impact Development (LID) approaches and raising the site elevation through additional fill are two potential adaptation options. Here, increasing the project site ground elevation by adding fill was evaluated as a possible option. Adding fill helps address the stormwater management system's deficiencies under future conditions by allowing to build the retention pond on higher ground, thus providing increased storage. In the first attempt, 15 cm of fill was applied, which increased the reliability of the stormwater pond to 89% (Figure 12). Although this is a significant improvement, the pond still fails to meet the ERP permitting criteria. Since Tampa Bay is listed as impaired waters, the increased reliability will be inadequate from a permitting standpoint. Adding 30 cm of fill will increase the reliability of the stormwater pond at the Tampa Bay project site, in future conditions, to 98% which is acceptable based on most permit regulations (Figure 12).

Figure 12. Pond water elevation under two different fill scenarios of 15 cm (6 inch) and 30 cm (1 foot) as adaptation options.

6. Conclusions

Florida has adopted stringent requirements for environmental protection and stormwater permitting. Despite this stringent policy, the results of this case study in the Tampa Bay area show that SLR and related groundwater effects may become a significant challenge for implementing flood protection measures in low-lying coastal areas. Currently, for most of permit studies, the climate data and boundary data are assumed to be stationary with respect to SLR. The simulation results demonstrate that SLR can substantially increase groundwater elevations and decrease in the soil storage capacity. In the presented case study, this change would double the discharge volume released from stormwater pond and increase the peak flow by about 50%. Although not covered in the

present analysis, stronger and more frequent recent tropical storms and hurricanes would further exacerbate the performance of stormwater retention ponds. The cumulative effects of peak flow increases reduced percolation from stormwater ponds in coastal communities can pose a significant challenge for existing primary drainage systems, which are designed for current conditions (or older). Therefore, more domestic road flooding should be expected toward the mid-century as a result of SLR-related groundwater rise alone. By the same token, under future conditions, there will be more incidents of retention ponds failing to recover treatment volumes within the required time period. These incidences will lead to release of untreated stormwater and could lead to environmental risks in the future unless plausible groundwater table rise scenarios are considered in the design and retrofit of retention ponds.

Author Contributions: Conceptualization, R.D., M.X.T., and A.M.; methodology, R.D. and A.M.; validation, R.D.; formal analysis, R.D.; writing—original draft preparation, R.D.; writing—technical review and editing, R.J.H., M.X.T., A.M. and K.M.; visualization, R.D.; supervision, M.X.T. and A.M. All authors have read and agreed to the published version of the manuscript.

Conflicts of Interest: The authors declare no conflict of interest.

References

1. IPCC. Summary for Policymakers. In *IPCC Special Report on the Ocean and Cryosphere in a Changing Climate*; Pörtner, H.-O., Roberts, D.C., Masson-Delmotte, V., Zhai, P., Tignor, M., Poloczanska, E., Mintenbeck, K., Nicolai, M., Okem, A., Petzold, J., et al., Eds.; IPCC Intergovernmental Panel on Climate Change: Geneva, Switzerland, 2019.

2. IPCC. Summary for policymakers. In *Climate Change 2014: Impacts, Adaptation, and Vulnerability. Part A: Global and Sectoral Aspects. Contribution of Working Group II to the Fifth Assessment Report of the Intergovernmental Panel on Climate Change*; Field, C.B., Barros, V.R., Dokken, D.J., Mach, K.J., Mastrandrea, M.D., Bilir, T.E., Chatterjee, M., Ebi, K.L., Estrada, Y.O., Genova, R.C., et al., Eds.; Cambridge University Press: Cambridge, UK; New York, NY, USA, 2014; pp. 1–32.

3. Masciopinto, C.; Serena, L.I. Assessment of the impact of sea-level rise due to climate change on coastal groundwater discharge. *Sci. Total Environ.* **2016**, *569*, 672–680. [CrossRef] [PubMed]

4. Melillo, J.M.; Richmond, T.T.C.; Yohe, G.W. (Eds.) Climate change impacts in the United States. In *The Third National Climate Assessment*; U.S. Global Change Research Program: Washington, DC, USA, 2014; 841p. [CrossRef]

5. Buenfil-López, L.A.; Rebollar-Plata, M.; Muñoz-Sevilla, N.P.; Juárez-León, B. Sea-Level rise and subsidence-Mexican South Pacific coast. *J. Coast. Res.* **2012**, *28*, 1154–1164. [CrossRef]

6. Perez, R.T.; Feir, R.B.; Carandang, E.; Gonzalez, E.B. Potential impacts of sea level rise on the coastal resources of Manila Bay: A preliminary vulnerability assessment. *Water Air Soil Pollut.* **1996**, *92*, 137–147.

7. Sojisuporn, P.; Sangmanee, C.; Wattayakorn, G. Recent estimate of sea-level rise in the Gulf of Thailand. *Maejo Int. J. Sci. Technol.* **2013**, *7*, 106–113.

8. Abi Suroso, D.S.; Kombaitan, B.; Setiawan, B. Exploring the use of risk assessment approach for climate change adaptation in Indonesia: Case study of flood risk and adaptation assessment in the South Sumatra province. *Procedia Environ. Sci.* **2013**, *17*, 372–381. [CrossRef]

9. Jato-Espino, D.; Sillanpaa, N.; Charlesworth, S.M. A simulation-optimization methodology to model urban catchments under non-stationary extreme rainfall events. *Environ. Model. Soft. Artic.* **2017**, in press. [CrossRef]

10. Hailegeorgis, T.T.; Alfredsen, K. Analyses of extreme precipitation and runoff events including uncertainties and reliability in design and management of urban water infrastructure. *J. Hydrol.* **2017**, *544*, 290–305. [CrossRef]

11. Zhang, K.; Manuelpillai, D.; Raut, B.; Deletic, A.; Bach, P.M. Evaluating the reliability of stormwater treatment systems under various future climate conditions. *J. Hydrol.* **2019**, *568*, 57–66. [CrossRef]

12. Nicholls, R.J. Planning for the impacts of sea level rise. *Oceanography* **2011**, *24*, 144–157. [CrossRef]

13. NOAA. Sea Level Trends. 2016. Available online: https://tidesandcurrents.noaa.gov/sltrends/sltrends.html (accessed on 20 December 2019).

14. NOAA. The Coastal Population Explosion. 2016. Available online: http://oceanservice.noaa.gov/websites/retiredsites/natdia_pdf/3hinrichsen.pdf (accessed on 20 December 2019).

15. NFIP. 2015. Available online: http://bsa.nfipstat.fema.gov/reports/1040.htm (accessed on 20 December 2019).

16. Climate Central. Available online: http://sealevel.climatecentral.org/ (accessed on 20 December 2019).

17. Milly, P.C.D.; Betancourt, J.; Falkenmark, M.; Hirsch, R.M.; Kundzewicz, Z.W.; Lettenmaier, D.P.; Stouffer, R.J. Stationarity is dead: Whither water management? *Science* **2008**, *319*, 573–574. [CrossRef]

18. Rui, H.; Herman, J.; Lund, J.; Madani, K. Adaptive water infrastructure planning for nonstationary hydrology. *Adv. Water Resour.* **2018**, *118*, 83–94.

19. Babovic, F.; Mijic, A.; Madani, K. Decision making under deep uncertainty for adapting urban drainage systems to change. *Urban Water J.* **2018**, *15*. [CrossRef]

20. LaRoche, T.B.; Webb, M.K. *Impact of Sea Level Rise on Stormwater Drainage Systems in the Charleston, South Carolina Area*; U.S. Environmental Protection Agency: Washington, DC, USA, 1978.

21. Parolari, A.J.; Pelrine, S.; Bartlett, M.S. Stochastic water balance dynamics of passive and controlled stormwater basins. *Adv. Water Resour.* **2018**, *122*, 328–339. [CrossRef]

22. Werner, A.D.; Simmons, C.T. Impact of sea-level rise on sea water Intrusion in coastal aquifers. *GroundWater* **2009**, *47*, 197–204. [CrossRef] [PubMed]

23. Joyce, J.; Chang, N.B.; Harji, R.; Ruppert, T.; Imen, S. Developing a multi-scale modeling system for resilience assessment of green-grey drainage infrastructures under climate change and sea level rise impact. *Environ. Model. Soft.* **2017**, *90*, 1–26. [CrossRef]

24. Czajkowski, J.; Engel, V.; Martinez, C.; Mirchi, A.; Watkins, D.; Sukop, M.C.; Hughes, J.D. Economic impacts of urban flooding in South Florida: Potential consequences of managing groundwater to prevent salt water intrusion. *Sci. Total Environ.* **2018**, *621*, 465–478. [CrossRef]

25. Southwest Florida Water Management District. Environmental Resource Permit Applicant's Handbook—Volume II—Design Requirements for Stormwater Treatment and Management Systems Water Quality and Water Quantity. 2018. Available online: https://www.swfwmd.state.fl.us (accessed on 20 December 2019).

26. Southwest Florida Water Management District. Guide to District Hydrologic Data. 2017. Available online: https://www.swfwmd.state.fl.us/sites/default/files/medias/documents/Guide_To_Hydrologic_Data_2017.pdf (accessed on 20 December 2019).

27. NOAA's National Weather Center. Available online: https://hdsc.nws.noaa.gov/ (accessed on 20 December 2019).

28. NRCS Digital Survey. Available online: https://websoilsurvey.sc.egov.usda.gov/App/WebSoilSurvey.aspx (accessed on 20 December 2019).

29. USDA-SCS. *Urban Hydrology for Small Watersheds*; Technical Release No. 55 (TR-55); USDASCS: Washington, DC, USA, 1986.

30. Streamline Technologies Inc. ICPR User Manual. Available online: www.streamnologies.com (accessed on 20 December 2019).

31. Chow, V.T. *Open-Channel Hydraulics*; McGraw-Hill: New York, NY, USA, 1959; 680p.

32. Green, W.H.; Ampt, G.A. Studies on soil physics, part 1, the flow of air and water through soils. *J. Agric. Sci.* **1911**, *4*, 11–24.

33. Chadwick, A.J.; Morfett, J.C. *Hydraulics in Civil and Environmental Engineering*; E & FN Spon: London, UK, 1993.

34. Hashimoto, T.; Stedinger, J.R.; Loucks, D.P. Reliability, resiliency and vulnerability criteria for water resource system performance evaluation. *Water Resour. Res.* **1982**, *18*, 14–20. [CrossRef]

35. Sandoval-Solis, S.; McKinney, D.C.; Loucks, D.P. Sustainability index for water resources planning and management. *J. Water Resour. Plan. Manag.* **2011**, *137*, 381–390. [CrossRef]

36. Gohari, A.; Mirchi, A.; Madani, K. System dynamics evaluation of climate change adaptation strategies for water resources management in central Iran. *Water Resour. Manag.* **2017**, *31*, 1413–1434. [CrossRef]

37. Jain, S.K.; Buynya, P.K. Reliability, resilience and vulnerability of a multipurpose storage reservoir. *Hydrol. Sci. J.* **2008**, *53*, 434–447. [CrossRef]

38. Lee, E.H.; Kim, J.H. Development of a reliability index considering flood damage for urban drainage systems. *KSCE J. Civ. Eng.* **2019**, *23*, 1872–1880. [CrossRef]

39. Davtalab, R.; Madani, K.; Massah, A.; Farajzadeh, M. Evaluating the effects of climate change on water reliability in Iran's Karkheh river basin. In Proceedings of the World Environmental and Water Resources Congress 2014, Portland, OR, USA, 1–5 June 2014; pp. 2127–2135.